Geomechanics and Engineering, *Vol. 17, No. 4 (2019) 385-392*
DOI: https://doi.org/10.12989/gae.2019.17.4.385

3D stress-fractional plasticity model for granular soil

Shunxiang Song[a], Yufeng Gao* and Yifei Sun[b]

Key Laboratory of Ministry of Education for Geomechanics and Embankment Engineering, College of Civil and Transportation Engineering, Hohai University, Nanjing 210098, China

(Received January 18, 2019, Revised February 26, 2019, Accepted March 5, 2019)

Abstract. The present fractional-order plasticity models for granular soil are mainly established under the triaxial compression condition, due to its difficult in analytically solving the fractional differentiation of the third stress invariant, e.g., Lode's angle. To solve this problem, a three dimensional fractional-order elastoplastic model based on the transformed stress method, which does not rely on the analytical solution of the Lode's angle, is proposed. A nonassociated plastic flow rule is derived by conducting the fractional derivative of the yielding function with respect to the stress tensor in the transformed stress space. All the model parameters can be easily determined by using laboratory test. The performance of this 3D model is then verified by simulating multi series of true triaxial test results of rockfill.

Keywords: fractional plastic flow rule; 3d stress state; transformed stress; state dependence

1. Introduction

The constitutive behavior of granular soil during plastic loading is nonassociated and state dependent (Yoshimoto *et al.* 2016, Chenari *et al.* 2018, Guliyev 2018, Kian *et al.* 2018, Oztoprak *et al.* 2018, Park *et al.* 2018, Sonmezer *et al.* 2018, Wu *et al.* 2018). Many different approaches, including the classic elastoplastic theory (Liu and Gao 2016, Liu *et al.* 2017 Tian and Yao 2017), hypoplastic model (Shi and Herle, 2016, 2017) and generalized elastoplastic theory (Pastor *et al.* 1990) etc., were introduced to capture this complex deformation mechanism. In these theories, the nonorthogonality between the plastic flow direction and yielding surface was usually modelled by introducing an additional assumption of a different plastic potential, which however could bring more parameters which may lack clear physical significances and thus impede its further application.

To overcome this limitation, a novel fractional viscoplasticity was proposed (Sumelka 2014, Sumelka and Nowak 2016), where the non-coaxiality between the loading and plastic flow directions can be easily simulated by conducting fractional derivative of the yielding function, where the additional plastic potential is no longer needed. Fractional plasticity can be used to describe the materials which have the behaviors of induced anisotropy and volume change in the plastic range. Therefore, this model can be applied for concrete, rock and granular soil by using proper strength criteria (Masoumi *et al.* 2015, Bui *et al.* 2016, Wang *et al.* 2018a, b, 2019). Then, a series of pioneering studies on establishing the fractional plasticity model for granular soils have been done by Sun and his co-workers (Sun and Shen 2017, Sun *et al.* 2017, Sun and Xiao 2017). In their studies, the fractional order was found to be capable of capturing both the state-dependence and the evolving plastic flow direction during shearing (Sun *et al.* 2017). However, the present fractional-order elastoplastic models for granular soils are all established at the triaxial compression state rather than the 3D stress state, so the stress-strain relationship under the true 3D stress condition cannot be described, which limits the further engineering application of these models, for example in railway engineering (Kumara and Hayano 2016, Mosayebi *et al.* 2016, Nimbalkar and Indraratna 2016, Nimbalkar *et al.* 2018). Hence, there is an urgent need to extend the fractional plasticity approach to cover more generalized stress conditions.

There are several methods proposed to generalize the constitutive models from 2D stress state to 3D stress state, for instance, the $g(\theta)$ method (Pastor *et al.* 1990) and t_{ij} method (Nakai and Hinokio, 2004). Besides, some specific stress spaces were introduced for the 3D generalization. For instance, the concepts of characteristic stress space (Lu *et al.* 2016, 2019) and transformed stress (TS) space (Yao and Wang, 2014). The concept of TS space was proposed by Yao and Wang (2014) to generalize the constitutive models for 3D loading conditions, which gained a lot of attention since emerging. Due to the integral definition of the fractional derivative, analytical solutions of the fractional derivative with respect to the Lode's angle cannot be easily obtained. However, in the TS method, such analytical solution is no longer needed; only conducting differentiations of the transformed mean effective principal stress and deviator stress are enough for accurate modelling of the 3D behaviour of soil.

*Corresponding author, Professor
E-mail: yfgao66@163.com
[a]Ph.D. Candidate
E-mail: songshunxiang0525@163.com
[b]Associate Professor
E-mail: sunny@hhu.edu.cn

http://www.techno-press.org/?journal=gae&subpage=7
ISSN: 2005-307X (Print), 2092-6219 (Online)

In this paper, a new elastoplastic model by combining the fractional plasticity and the TS method is established, where a novel 3D plastic flow rule is derived by conducting stress-fractional derivative of the yielding function in the TS space. Available true triaxial test results of the Lianghekou rockfill (Shi, 2008) are used to validate the performance of this new 3D fractional-order elastoplastic model.

2. Fractional derivative

In this study, the Caputo's derivative (Podlubny 1998) of a yielding function, *f*, is used

$$ {}_0D_\sigma^\alpha f(\sigma) = \frac{1}{\Gamma(n-\alpha)} \int_0^\sigma \frac{f^{(n)}(\chi)}{(\sigma-\chi)^{\alpha+1-n}} d\chi, \quad \sigma > 0 \tag{1} $$

where ${}_0D_\sigma^\alpha (= \partial^\alpha / \partial\sigma^\alpha)$ means the partial differentiation, and $\alpha \in (0, 2)$, is the fractional derivative order (Sun *et al.*, 2019). Note that there are a variety of definitions of the fractional derivative (Podlubny, 1998); however, for modelling the strain hardening and softening behaviour of soil using plasticity approach, the Caputo's definition is preferred (Sun *et al.*, 2017), because of its derivative of a constant equal to zero. σ is the loading stress. It should be noted that compressive stresses and strains are considered as positive while the extensive ones are negative; all the stresses in this paper are effective stresses unless otherwise specified. The Euler Gamma function is defined as $\Gamma(x) = \int_0^\infty e^{-\tau}\tau^{x-1}d\tau$. Hence, the explicit expression of the Caputo's derivative of a power function, x^v, can be obtained as

$$ {}_0D_x^\alpha (x^v) = \frac{\partial^\alpha (x^v)}{\partial x^\alpha} = \frac{\Gamma(v+1)}{\Gamma(v+1-\alpha)} x^{v-\alpha} \tag{2} $$

where v>-1, is the power index. As will be shown in the next section, with the use of a fractional oder ($\alpha \neq 1$), a state-dependent nonassociated plastic flow rule can be achieved.

3. Transformed stress space

According to Yao and Wang (2014), the TS method requires an arbitrary failure criterion. In this paper, the SMP criterion (Matsuoka *et al.* 1999) is used. Then, the TS space ($\tilde{\sigma}_{ij}$, i, j = 1, 2, 3) can be constructed by using the TS tensor $\tilde{\sigma}_{ij}$. The SMP criterion in the general stress space (σ_{ij}) will be transformed into the extended Mises criterion in the TS space. As shown in Fig. 1, the curve of the SMP criterion in the original π–plane can be transformed into a circle in the new transformed π–plane, which indicates that the effect of Lode's angle in the TS space can be neglected.

In addition, it can be observed from Fig. 2 that the yielding surface (*f*) of the modified Cam-clay (MCC) model in the TS space have the same shape with that of the MCC model using extended Mises criterion. Therefore, further fractional derivatives of *f* can be only carried out with respect to the mean effective principal stress and deviator stress in the TS space.

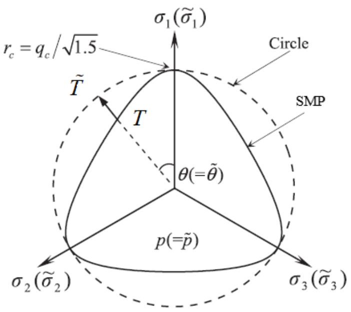

Fig. 1 Transformation from the general space to the transformed space

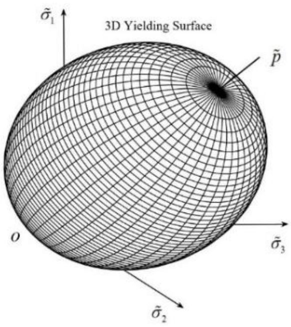

Fig. 2 Yielding surface of the MCC model in the TS space

The transformation from the σ_{ij} space to the $\tilde{\sigma}_{ij}$ space (point T to point $\tilde{T}$ in Fig. 1) can be obtained via the deviator stress q_c under the triaxial compression condition (Yao and Wang 2014), such that

$$ \tilde{p} = p \tag{3a} $$

$$ \tilde{q} = q_c \tag{3b} $$

$$ \tilde{b} = b \text{ or } \tilde{\theta} = \theta \tag{3c} $$

where p and θ are the mean effective principal stress and the Lode's angle in the σ_{ij} space, respectively. The expressions of the transformed mean effective principal stress $\tilde{p}$, deviator stress $\tilde{q}$, and intermediate principal stress coefficient $\tilde{b}$ in the TS space have the same forms as those in the general stress space

$$ \tilde{p} = \frac{1}{3}\tilde{\sigma}_{ii} \tag{4a} $$

$$ \tilde{q} = \sqrt{\frac{3}{2}\tilde{s}_{ij}\tilde{s}_{ij}} \tag{4b} $$

$$ \tilde{s}_{ij} = \tilde{\sigma}_{ij} - \tilde{p}\delta_{ij} \tag{4c} $$

$$ \tilde{b} = \frac{\tilde{\sigma}_2 - \tilde{\sigma}_3}{\tilde{\sigma}_1 - \tilde{\sigma}_3} \tag{4d} $$

where $\tilde{s}_{ij}$ is the deviator stress tensor in the $\tilde{\sigma}_{ij}$ space; and δ_{ij} is the Kronecker delta. Based on the SMP criterion (Matsuoka *et al.* 1999), q_c can be expressed as

$$q_c = \frac{2I_1}{3\sqrt{(I_1 I_2 - I_3)/(I_1 I_2 - 9I_3)} - 1} \tag{5}$$

where I_1, I_2, and I_3 are the stress invariants in the σ_{ij} space, which can be expressed as

$$I_1 = \sigma_{ii} \tag{6a}$$

$$I_2 = \frac{1}{2}(\sigma_{kk})^2 - \frac{1}{2}\sigma_{ij}\sigma_{ji} \tag{6b}$$

$$I_3 = \frac{1}{3}\sigma_{ij}\sigma_{jk}\sigma_{ki} - \frac{1}{2}\sigma_{rs}\sigma_{sr}\sigma_{mm} + \frac{1}{6}(\sigma_{nn})^3 \tag{6c}$$

Then, the TS tensor ($\tilde{\sigma}_{ij}$) can be obtained as

$$\tilde{\sigma}_{ij} = \begin{cases} p\delta_{ij} + \dfrac{q_c}{q}\left(\sigma_{ij} - p\delta_{ij}\right), & (q \neq 0) \\ \sigma_{ij}, & (q = 0) \end{cases} \tag{7}$$

Based on the mathematical relationship between $\tilde{\sigma}_{ij}$ and σ_{ij}, the 3D constitutive model can be established directly in the TS space and then transferred in the ordinary stress space during calculation.

4. 3D fractional model

The total strain ε_{ij} and its increment $\Delta\varepsilon_{ij}$ can be divided into two parts, such that

$$\Delta\varepsilon_{ij} = \Delta\varepsilon_{ij}^e + \Delta\varepsilon_{ij}^p \tag{8}$$

where the superscripts e and p indicate the elastic and plastic components, respectively. Following the fractional plasticity (Sun and Shen 2017, Sun *et al.* 2017), the plastic strain increment is determined by using the stress-fractional derivative of f, such that

$$\Delta\varepsilon_{ij}^p = \Lambda \frac{\partial^\alpha f(\sigma)}{\partial \sigma_{ij}^\alpha} \tag{9}$$

where Λ is the non-negative plastic multiplier. $\partial^\alpha f(\sigma)/\partial\sigma_{ij}^\alpha$ indicates the direction of nonassociated plastic flow. As shown in Fig. 3, the solid line n which is orthogonal to f denotes the loading direction, while the flow direction (dashed line m) is not orthogonal to f due to the ability of the fractional derivative to adjust the gradient direction. The extent of non-coaxiality is determined by α. When $\alpha = 1$, the plastic flow rule will be associated.

The well-known MCC yielding function (Schofield and Wroth 1968) is defined as

$$f = M^2\tilde{p}^2 + \tilde{q}^2 - M^2\tilde{p}_0\tilde{p} = 0 \tag{10}$$

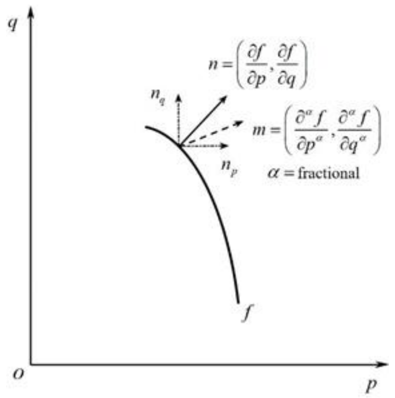

Fig. 3 The non-coaxiality between the loading and flow directions

where M ($= 6\sin\phi_c/(3-\sin\phi_c)$) is the critical-state stress ratio; ϕ_c denotes the critical-state friction angle at triaxial compression. To obtain the value of ϕ_c, at least three independent triaxial compression tests on granular soils, under different confining pressures, needs to be carried out. Then, one can plot the critical state data points in the p–q plane, from which the value of M can be obtained. Then, the value of ϕ_c can be obtained by using $\phi_c = \arctan[3M/(6+M)]$. $\tilde{p}_0$ is the intercept between f and the abscissa in the $\tilde{p}-\tilde{q}$ plane. Then, the following constitutive relation can be achieved (Sun and Xiao 2017)

$$\Delta\varepsilon_{ij}^p = \frac{1}{\Pi} m_{ij} n_{kl} \Delta\sigma_{kl} \tag{11}$$

where $\prod$ denotes the hardening modulus. m_{ij} and n_{kl} denote the flow direction and loading direction, respectively. According to Yao and Wang (2014), n_{kl} can be defined as

$$n_{kl} = \frac{\dfrac{\partial f}{\partial \sigma_{kl}}}{\sqrt{\dfrac{\partial f}{\partial \sigma_{rs}}\dfrac{\partial f}{\partial \sigma_{rs}}}} \tag{12}$$

where $\partial f/\partial\sigma_{kl}$ based on the TS method is defined as

$$\frac{\partial f}{\partial \sigma_{kl}} = \begin{cases} \dfrac{\partial f}{\partial \tilde{\sigma}_{mn}}\dfrac{\partial \tilde{\sigma}_{mn}}{\partial \sigma_{kl}}, & (q \neq 0) \\ \dfrac{\partial f}{\partial \tilde{\sigma}_{kl}}, & (q = 0) \end{cases} \tag{13}$$

where

$$\begin{aligned} \frac{\partial \tilde{\sigma}_{mn}}{\partial \sigma_{kl}} &= \frac{1}{3}\delta_{kl}\delta_{mn} + \frac{s_{mn}}{q}\frac{\partial q_c}{\partial \sigma_{kl}} \\ &+ \frac{q_c}{q}\left(\delta_{km}\delta_{ln} - \frac{1}{3}\delta_{kl}\delta_{mn} - \frac{3}{2q^2}s_{kl}s_{mn}\right) \end{aligned} \tag{14}$$

$$\frac{\partial q_c}{\partial \sigma_{kl}} = \sum_{t=1}^{3}\frac{\partial q_c}{\partial I_t}\frac{\partial I_t}{\partial \sigma_{kl}} \tag{15}$$

where the definition of $\partial q_c / \partial I_t$ and $\partial I_t / \partial \sigma_{kl}$ can be found in the appendix. Furthermore, m_{ij} can be defined as (Sun *et al.* 2017)

$$m_{ij} = \frac{\dfrac{\partial^\alpha f}{\partial \tilde{\sigma}_{ij}^\alpha}}{\sqrt{\dfrac{\partial^\alpha f}{\partial \tilde{\sigma}_{kl}^\alpha}\dfrac{\partial^\alpha f}{\partial \tilde{\sigma}_{kl}^\alpha}}} \tag{16}$$

where $\partial^\alpha f / \partial \tilde{\sigma}_{ij}^\alpha$ can be derived by conducting the fractional derivative of f

$$\frac{\partial^\alpha f}{\partial \tilde{\sigma}_{ij}^\alpha} = \frac{\tilde{\sigma}_{ij}^{1-\alpha}}{\Gamma(2-\alpha)}\left(A\tilde{\sigma}_{ij} + B\right) \tag{17}$$

$$A = \frac{2M^2(\alpha-1)}{9(2-\alpha)} + \frac{4-\alpha}{2-\alpha} \tag{18a}$$

$$B = \frac{M^2\tilde{p}^2 - \tilde{q}^2}{3\tilde{p}} - 3\tilde{p} \tag{18b}$$

As shown in Eqs. (16) and (17), the flow direction is influenced by α. A non-associated flow rule can be obtained even without using an additional plastic potential. Meanwhile, many studies pointed out that the material state can affect the flow direction. Therefore, the following expression of α which describes the state-dependence of nonassociated plastic flow is used (Sun and Xiao 2017)

$$\alpha = e^{\beta\psi} \tag{19}$$

where $\beta > 0$, is a material constant. In classical plasticity, the first-order derivative of the yielding function is used to obtain a normal vector where the associated plastic flow direction is implied. This viewpoint can help us to understand the meaning of β, which represents the state-dependent non-associativity in plasticity. The state parameter, $\psi=e-e_c$ (Been and Jefferies 1985), where e and e_c are the void ratios at the current and critical states, respectively. $e_c = e_\Gamma - \lambda(p/p_a)^\xi$, where e_Γ, λ and ξ are three critical-state parameters in the $e-p$ plane (Li and Wang, 1998). In addition, the following modified hardening modulus, $\prod$, proposed by Li and Dafalias (2000) is used

$$\Pi = (h_1 - h_2 e)G\left(\frac{M_p}{\tilde{\eta}} - 1\right)e^{k\psi} \tag{20}$$

where $\tilde{\eta} = \tilde{q}/\tilde{p}$ is the stress ratio in the TS space. h_1 and h_2 are material constants, which can describe the dependence of the hardening parameter on void ratios. The parameters h_1 and h_2 can be determined by fitting the relationship of soils with different initial conditions. After the calibration the values of h, the relationship between h and e can be obtained. Then, the constants h_1 and h_2 can be determined. The characteristic peak stress ratio, $M_p=M_e^{-k\psi}$, where k is a material constant. G is the shear modulus

$$G = G_0 \frac{(2.97-e)^2}{1+e} p_a \sqrt{\frac{p'}{p_a}} \tag{21}$$

Table 1 Model parameters

Soil	ϕ_c	λ	e_Γ	ξ	β	k	h_1	h_2	G_0	v
Rockfill G1	46°	0.11	0.404	0.1	0.2	0.1	1.2	0.3	90	0.25
Rockfill G2	51°	0.024	0.314	0.3	0.6	0.3	0.6	0.1	90	0.25

Table 2 Gradation parameters of two rockfills

Soil	C_u	C_c	d_{50} (mm)	d_{max} (mm)	d_{min} (mm)
Rockfill G1	1.59	0.95	3.15	5	2
Rockfill G2	22.67	12.25	6.10	10	0.075

where G_0 is a dimensionless elastic constant. Apart from the plastic deformation, the elastic deformation of soils should be also considered, such that

$$\Delta\varepsilon_{ij}^e = C_{ijkl}^e \Delta\sigma_{kl} \tag{22}$$

where the elastic compliance matrix C^e_{ijkl} is defined as

$$C_{ijkl}^e = \begin{cases} \dfrac{1}{2G(1+\nu)}, & i=j \\ \dfrac{-\nu}{2G(1+\nu)}, & i \neq j \end{cases} \tag{23}$$

where v is the Poisson's ratio. Then, by using Eqs. (11), and (22), the 3D fractional elastoplastic constitutive relationship can be obtained. In this study, there are totally ten parameters (ϕ_c, λ, e_Γ, ξ, β, k, h_1, h_2, G_0 and v). In this model, all the parameters can be determined by traditional triaxial tests. This is an advantage of the TS method which does not require additional parameters under true triaxial condition. All the parameters are inherited from triaxial condition. This concept has been comprehensively discussed in Yao *et al.* (2014) and thus not repeated here for simplicity. Details for obtaining each model parameter can be found in Sun and Xiao (2017), and thus not repeated here for simplicity. Table 1 lists the values of each model parameters used for numerical simulation.

5. Model validation

In this section, the performance of the 3D fractional elastoplastic model in simulating soil deformation is evaluated. Test results of the Lianghekou rockfill (Shi 2008) with two different gradations (i.e., G1 and G2) under different true 3D stress conditions are used. The particle distributions of the two rockfills are shown in Fig. 4. Model predictions of each test result can be found in Figs. 5 and 6.

It was reported (Shi 2008) that the size of the cuboid true triaxial sample was 70 mm × 70 mm × 35 mm. All the tests were carried out under the loading path of $\Delta\sigma_3= 0$ with varying b values. As can be observed, test results under three different values of b were used for model prediction. The dry density (ρ_d) of rockfill G1 was reported to be 1.43 g/cm^3 while the minimum particle size and maximum particle size were 2 mm and 5 mm, respectively. The ρ_d of rockfill G2 was tested to be 1.91 g/cm^3. It was reported that

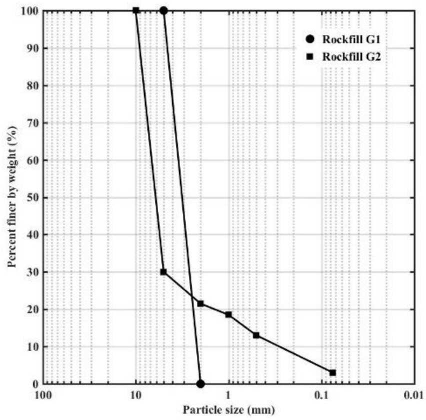

Fig. 4 Particle size distribution (data sourced from Shi (2018))

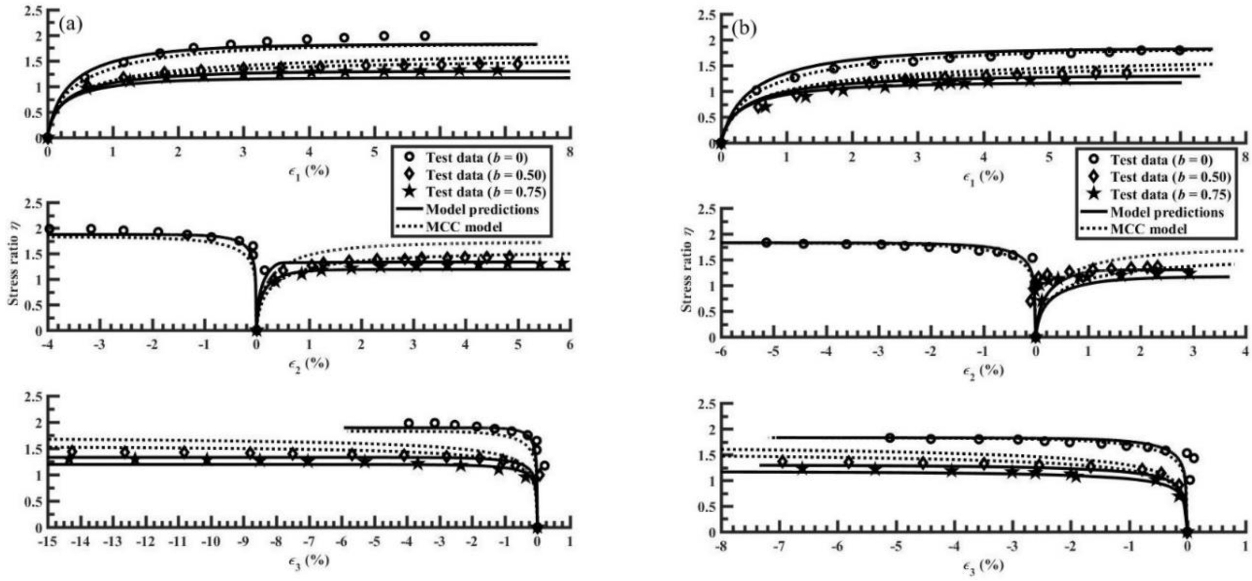

(a) σ_3= 100 kPa (b) σ_3= 200 kPa

Fig. 5 Comparisons between the test data of the rockfill G1 and the prediction of the proposed model

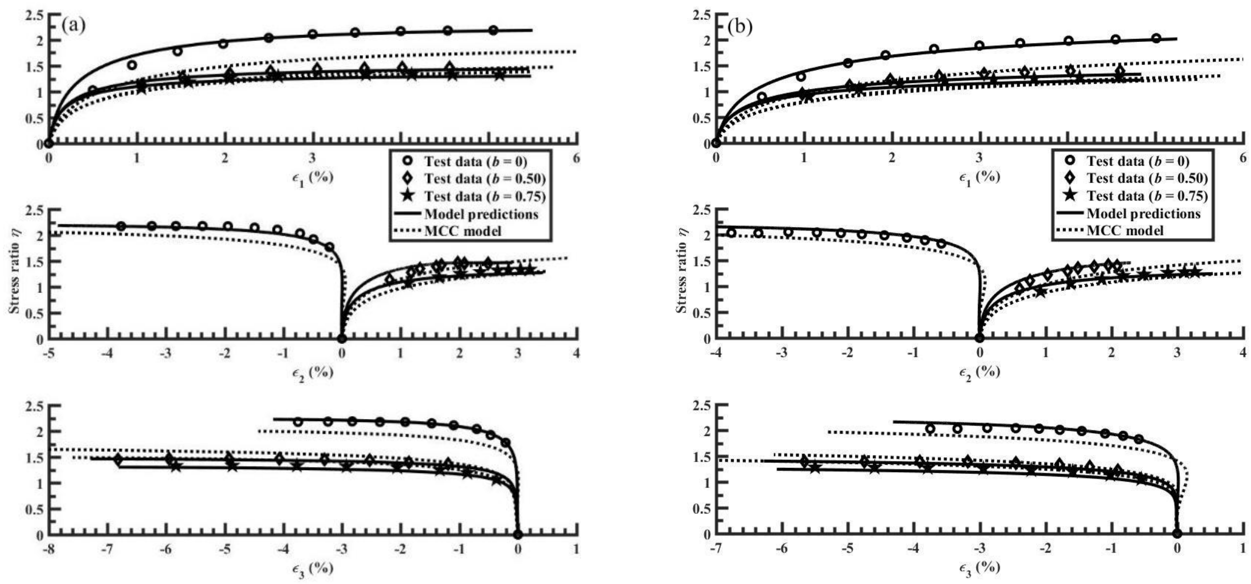

(a) σ_3= 200 kPa (b) σ_3= 400 kPa

Fig. 6 Comparisons between the test data of the rockfill G2 and the prediction of the proposed model

70% particles of rockfill G2 had sizes of 5 mm to 10 mm while the rest were less than 5 mm. The relations between the principal strains (ε_i) and the stress ratio ($\eta=q/p$) predicted by the proposed 3D model are indicated by solid lines, as shown in Figs. 5 and 6, while the true triaxial test results of Lianghekou rockfill are indicated by discrete symbols. Comparisons between the simulations and the test data show that the proposed 3D fractional elastoplastic model can well capture the stress-strain behaviour of different rockfill materials under different true triaxial loading conditions. In addition, compared with the MCC model, the proposed model can capture the stress-strain relationship more accurately.

The influence of intermediate principal stress coefficients can be also predicted better than the MCC model. During loading under different σ_3, b maintains constant, while b = 0, 0.5, and 0.75, respectively. It can be observed that η increases with the increase of the first principal strain (ε_1), and only when it is at the triaxial compression state (b = 0), the values of the second principal strain (ε_2) is negative, i.e., extensive, while the third principal strain (ε_3) is extensive all the time. In addition, ε_1 is greater than ε_2 and ε_3 when b is small; but, with the increase of b, the ε_1 becomes smaller than ε_2 and ε_3.

6. Conclusions

In this paper, a 3D fractional-order constitutive model based on the fractional plasticity theory and the TS method was proposed. The main findings in this study are summarized as follows:

(1) A 3D state-dependent non-associated plastic flow rule was obtained without using an additional plastic potential. The plastic flow direction was determined by performing fractional derivative of the yielding function while the loading direction was determined by taking the first-order derivative of the yielding function. The property of non-associativity can be simulated by only using a yielding surface, due to the ability of the fractional derivative to adjust gradient directions.

(2) The model can capture the state-dependence by combining the state parameter (β) and the fractional order (α). Based on the TS method, the hardening modulus was modified, so that it can reflect the property of hardening under 3D stress state. Meanwhile, all the model parameters used in this model can be determined by traditional triaxial tests.

(3) The performance of this model was verified through comparisons between the model predictions and true triaxial test results of two rockfill materials, from which a good model performance was observed.

(4) At current stage, the cyclic loading cannot be simulated in this model, as the loading and unloading behaviours should be defined by both the left-sided and right-sided fractional derivative. Meanwhile, the extension and rotational loading of this model also needs to be carried out to improve the ability of simulating more constitutive behaviours. Furthermore, the work of the combination of the proposed model and some business software should be done in the future study.

Acknowledgements

The financial supports provided by the National Natural Science Foundation of China (Grant Nos. 41630638, 51679068), the National Key Basic Research Program of China ("973" Program) (Grant No. 2015CB057901), the Fundamental Research Funds for the Central Universities (Grant No. 2017B05214) and the Project funded by China Postdoctoral Science Foundation (Grant No. 2017M621607) are greatly appreciated. The third author would also like to express his sincere gratitude to Prof. Wen Chen, in Hohai University, for his invaluable inspiration on the application of fractional calculus.

References

Been, K. and Jefferies, M.G. (1985), "A state parameter for sands", *Géotechnique*, **35**(2), 99-112.

Bui, T.A., Wong, H., Deleruyelle, F. and Zhou, A. (2016), "Constitutive modelling of the time-dependent behaviour of partially saturated rocks", *Comput. Geotech.*, **78**, 123-133.

Chenari, C.J., Fatahi, B., Ghorbani, A. and Alamoti, M.N. (2018), "Evaluation of strength properties of cement stabilized sand mixed with EPS beads and fly ash", *Geomech. Eng.*, **14**(6), 533-544.

Guliyev, H.H. (2018), "Geomechanical analysis of elastic parameters of the solid core of the Earth", *Geomech. Eng.*, **14**(1), 19-27.

Kian, A.R.T., Zakeri, J.A. and Sadeghi, J. (2018), "Experimental investigation of effects of sand contamination on strain modulus of railway ballast", *Geomech. Eng.*, **14**(6), 563-570.

Kumara, J.J. and Hayano, K. (2016), "Importance of particle shape on stress-strain behaviour of crushed stone-sand mixtures", *Geomech. Eng.*, **10**(4), 455-470.

Li, X. and Dafalias, Y. (2000), "Dilatancy for cohesionless soils", *Géotechnique*, **50**(4), 449-460.

Li, X. and Wang, Y. (1998), "Linear representation of steady-state line for sand", *J. Geotech. Geoenviron. Eng.*, **124**(12), 1215-1217.

Liu, M. and Gao, Y. (2016), "Constitutive modeling of coarse-grained materials incorporating the effect of particle breakage on critical state behavior in a framework of generalized plasticity", *Int. J. Geomech.*, **17**(5), 04016113.

Liu, M., Zhang, Y. and Zhu, H. (2017), "3D elastoplastic model for crushable soils with explicit formulation of particle crushing", *J. Eng. Mech.*, **143**(12), 04017140.

Lu, D., Liang, J., Du, X., Ma, C. and Gao, Z. (2019), "Fractional elastoplastic constitutive model for soils based on a novel 3D fractional plastic flow rule", *Comput. Geotech.*, **105**, 277-290.

Lu, D., Ma, C., Du, X., Jin, L. and Gong, Q. (2016), "Development of a new nonlinear unified strength theory for geomaterials based on the characteristic stress concept", *Int. J. Geomech.*, **17**(2), 04016058.

Masoumi, H., Douglas, K. and Russell, A. (2015), "A bounding surface plasticity model for intact rock exhibiting size-dependent behaviour", *Rock Mech. Rock Eng.*, **49**(1), 47-62.

Matsuoka, H., Yao, Y. and Sun, D. (1999), "The cam-clay models revised by the SMP criterion", *Soils Found.*, **39**(1), 81-95.

Mosayebi, S., Zakeri, J. and Esmaeili, M. (2016), "A comparison between the dynamic and static stiffness of ballasted track: A field study", *Geomech. Eng.*, **11**(6), 757-769.

Nakai, T. and Hinokio, M. (2004), "A simple elastoplastic model for normally and over consolidated soils with unified material parameters", *Soils Found.*, **44**(2), 53-70.

Nimbalkar, S. and Indraratna, B. (2016), "Improved performance of ballasted rail track using geosynthetics and rubber shockmat", *J. Geotech. Geoenviron. Eng.*, **142**(8), 04016031.

Nimbalkar, S., Annapareddy, V.S.R. and Pain, A. (2018), "A simplified approach to assess seismic stability of tailings dams", *J. Rock Mech. Geotech. Eng.*, **10**(6), 1082-1090.

Oztoprak, S., Sargin, S., Uyar, H.K. and Bozbey, I. (2018), "Modeling of pressuremeter tests to characterize the sands", *Geomech. Eng.*, **14**(6), 509-517.

Park, T., Kim, H., Tanvir, M., Lee, J. and Moon, S. (2018), "Influence of coarse particles on the physical properties and quick undrained shear strength of fine-grained soils", *Geomech. Eng.*, **14**(1), 99-105.

Pastor, M., Zienkiewicz, O.C. and Chan, A.H.C. (1990), "Generalized plasticity and the modelling of soil behavior", *Int. J. Numer. Anal. Meth. Geomech.*, **14**(3), 151-190.

Podlubny, I. (1998), *Fractional Differential Equations: An Introduction to Fractional Derivatives, Fractional Differential Equations, to Methods of Their Solution and Some of Their Applications*, Academic Press, San Diego, California, U.S.A.

Schofield, A. and Wroth, P. (1968), *Critical State Soil Mechanics*, McGraw-Hill London, U.K.

Shi, W.C. (2008), "True triaxial tests on coarse-grained soils and study on constitutive model", Ph.D., Hohai University, Nanjing, China.

Shi, X.S. and Herle, I. (2016), "Analysis of the compression behavior of artificial lumpy composite materials", *Int. J. Numer. Anal. Meth. Geomech.*, **40**(10), 1438-1453.

Shi, X.S. and Herle, I. (2017), "Numerical simulation of lumpy soils using a hypoplastic model", *Acta Geotech.*, **12**(2), 349-363.

Sonmezer, Y.B., Bas, S., Isik, N.S. and Akbas, S.O. (2018), "Linear and nonlinear site response analyses to determine dynamic soil properties of Kirikkale", *Geomech. Eng.*, **16**(4), 435-448.

Sumelka, W. (2014), "Fractional viscoplasticity", *Mech. Res. Commun.*, **56**, 31-36.

Sumelka, W. and Nowak, M. (2016), "Non-normality and induced plastic anisotropy under fractional plastic flow rule: A numerical study" *Int. J. Numer. Anal. Meth. Geomech.*, **40**(5), 651-675.

Sun, Y. and Shen, Y. (2017), "Constitutive model of granular soils using fractional order plastic flow rule", *Int. J. Geomech.*, **17**(8), 04017025.

Sun, Y. and Xiao, Y. (2017), "Fractional order plasticity model for granular soils subjected to monotonic triaxial compression", *Int. J. Solids Struct.*, **118**, 224-234.

Sun, Y., Gao, Y. and Chen, C. (2019), "Critical-state fractional model and its numerical scheme for isotropic granular soil considering state-dependence", *Int. J. Geomech.*, **13**(9), 04018202.

Sun, Y., Song, S., Xiao, Y. and Zhang, J. (2017), "Development and application of state-dependent fractional plasticity in modeling the non-associated behavior of granular aggregates", *Acta Mech. Solida Sin.*, **30**(5), 507-519.

Tian, Y. and Yao, Y.P. (2017), "A simple method to describe three-dimensional anisotropic failure of soils", *Comput. Geotech.*, **92**, 210-219.

Wang, W., Martin, P.R., Sheikh, M.N. and Hadi, M.N. (2018a), "Eccentrically loaded FRP confined concrete with different wrapping schemes", *J. Compos. Construct.*, **22**(6), 04018056.

Wang, W., Sheikh, M.N., Al-Baali, A.Q. and Hadi, M.N.S. (2018b), "Compressive behaviour of partially FRP confined concrete: Experimental observations and assessment of the stress-strain models", *Construct. Build. Mater.*, **192**, 785-797.

Wang, W., Wu, C. and Liu, Z. (2019), "Compressive behavior of hybrid double-skin tubular columns with ultra-high performance fiber-reinforced concrete (UHPFRC)", *Eng. Struct.*, **180**, 419-441.

Wu, Y., Hyodo, M. and Aramaki, M. (2018), "Undrained cyclic shear characteristics and crushing behaviour of silica sand", *Geomech. Eng.*, **14**(1), 1-8.

Yao, Y. and Wang, N. (2014), "Transformed stress method for generalizing soil constitutive models", *J. Eng. Mech.*, **140**(3), 614-629.

Yoshimoto, N., Wu, Y., Hyodo, M. and Nakata, Y. (2016), "Effect of relative density on the shear behaviour of granulated coal ash", *Geomech. Eng.*, **10**(2), 207-224.

CC

Appendix

According to Yao and Wang (2014), $\partial q_c / \partial I_t$ (t = 1, 2, 3) can be derived as

$$\frac{\partial q_c}{\partial I_1} = \frac{6\sqrt{\frac{\left(I_1 I_2 - I_3\right)}{\left(I_1 I_2 - 9I_3\right)}} + \frac{24 I_1 I_2 I_3}{\sqrt{\left(I_1 I_2 - I_3\right) / \left(I_1 I_2 - 9I_3\right)^3}} - 2}{\left(3\sqrt{\left(I_1 I_2 - I_3\right) / \left(I_1 I_2 - 9I_3\right)} - 1\right)^2} \tag{A1}$$

$$\frac{\partial q_c}{\partial I_2} = \frac{24 I_1^2 I_3 \Big/ \sqrt{\left(I_1 I_2 - I_3\right)\left(I_1 I_2 - 9I_3\right)^3}}{\left[3\sqrt{\left(I_1 I_2 - I_3\right) / \left(I_1 I_2 - 9I_3\right)} - 1\right]^2} \tag{A2}$$

$$\frac{\partial q_c}{\partial I_3} = \frac{-24 I_1^2 I_2 \Big/ \sqrt{\left(I_1 I_2 - I_3\right)\left(I_1 I_2 - 9I_3\right)^3}}{\left[3\sqrt{\left(I_1 I_2 - I_3\right) / \left(I_1 I_2 - 9I_3\right)} - 1\right]^2} \tag{A3}$$

while $\partial I_t / \partial \sigma_{kl}$ is expressed as

$$\frac{\partial I_1}{\partial \sigma_{kl}} = \delta_{kl} \tag{A4}$$

$$\frac{\partial I_2}{\partial \sigma_{kl}} = I_1 \delta_{kl} - \sigma_{kl} \tag{A5}$$

$$\frac{\partial I_3}{\partial \sigma_{kl}} = \left(\sigma_{kl}\right)^2 - I_1 \delta_{kl} + I_2 \delta_{kl} \tag{A6}$$

where k, l = 1, 2, 3. For more details of Eqs. (A1)-(A6), one can refer to Yao and Wang (2014).